Theoretical modelling of alpha particle-induced X-ray signals from the lunar surface

The elemental composition of a planetary surface can be deduced from *in situ* measurements by remote sensing techniques or laboratory analysis of the returned samples. Compositional maps of the moon, Mars and asteroids have been obtained using remote sensing X-ray[1] and gamma-ray[2] spectroscopy in the last six decades of planetary exploration. With respect to lunar science, the magnesium number, i.e. MgO/(MgO + FeO) estimation is considered significant for understanding lunar origin. Determination of the abundance of major elements in the South Pole Aitkin Basin at high spatial resolution will improve our knowledge regarding the early evolution of the moon[3].

X-ray fluorescence (XRF) technique involves the emission of characteristic X-rays due to the transfer of energy involved when the orbital electrons of an element are reorganized after electrons are ejected by an excitation process[1,4–7]. Since the moon does not have an atmosphere, solar X-rays excite atoms on the surface and produce X-ray lines, with signal intensities dependent on the elemental composition and solar activity levels[1,5]. Banerjee and Vadawale[7] have previously determined XRF signals observable by a 14 cm^2 X-ray detector from a 100 km lunar orbit. While Mg, Al and Si K_α lines were detected for all solar conditions, Ca, Ti and Fe K_α line signals were detectable when the solar X-ray spectra 'hardened' (i.e. larger output at higher X-ray energies) during M and X flare conditions[1].

Alpha particle-induced X-ray spectroscopy (APXS) measures characteristic X-ray lines emitted by atoms excited by incident alpha and X-ray radiation. APXS has been used to determine the composition of the Martian surface during the Mars Pathfinder mission, Mars Exploration Rovers in 2003 and Mars Science Laboratory in 2013 (refs 8, 9). APXS was also flown on-board the Chandrayaan-2 rover Pragyaan[10]. This study presents a novel method for estimating the anticipated APXS signals from prominent K_α lines for various lunar compositions (KREEP basalt and FAN considered here), assuming a silicon drift X-ray detector (SDD) of 30 mm^2 area, with an energy resolution of ~150 eV at 5.9 keV. The alpha irradiation source is assumed to be ^{244}Cm, with a total activity of ~30 mCi. The ^{244}Cm source emits alpha particles with an energy of 5.8 MeV and several X-ray lines, including the prominent ones occurring at 14.3 and 18.3 keV.

Assuming that the sample has a homogeneous interior and is much thicker than the total interaction length, the characteristic K_α X-ray line intensity produced from X-ray fluorescence is expressed as[4]

$$I = C_j \omega_j g_j \frac{r_j - 1}{r_j} \frac{\Omega}{4\pi D^2} \times \int_{\lambda_{\min}}^{\lambda_{\text{edg}}} J(\lambda)\cos(\alpha) \times \frac{\mu_j(\lambda)\mathrm{d}\lambda}{\sum_i [C_i \mu_i(\lambda) + C_i \mu_i(\lambda_j)\cos\alpha/\cos\beta]}. \quad (1)$$

Details of parameters and estimation of background signal due to coherent and incoherent scattering of X-rays have been described previously by Clark and Trombka[1].

For particle (e.g. proton or alpha particle)-induced K_α X-ray lines, Clayton *et al.*[11] suggested that the intensity of the X-ray photon signal can be expressed as

$$I = C \frac{N}{W} \frac{\Omega}{4\pi} \times \varepsilon \times F \times \int \frac{\mathrm{d}E}{S(E)} \sigma \exp\left(-\mu \int \frac{\mathrm{d}E}{S(E)} \frac{\cos\alpha}{\cos\beta} \right), \quad (2)$$

where C is the concentration of the element, N the Avogadro number, W the atomic mass, F the total particle (proton) charge irradiated on the target, S the matrix composite stopping power, ε the detector efficiency, σ the X-ray production cross-section for the element, μ the composite mass attenuation factor of the matrix, Ω the solid angle of the detector and α and β are the angle of particle beam with respect to the matrix normal and angle of the detector with respect to the matrix normal respectively. We have used eq. (2) to estimate the alpha-induced X-ray signal on the lunar surface for K_α signals from Al, Si, Mg, Ca, Ti and Fe. Table 1 presents the elemental concentrations, while the respective

Table 1. Elemental concentration (wt%) for KREEP basalt, high Al basalt and FAN composition used in the calculations

Oxide	Concentration		
	KREEP basalt	FAN	High Al basalt
MgO	7.8	0.26	8.5
Al_2O_3	16.9	35.6	13.6
SiO_2	52.5	44.5	46.4
CaO	9.4	20.4	11.2
TiO_2	1.9	0.02	2.6
FeO	9.02	0.21	16.8
Na_2O	0.87	0.36	0.0001

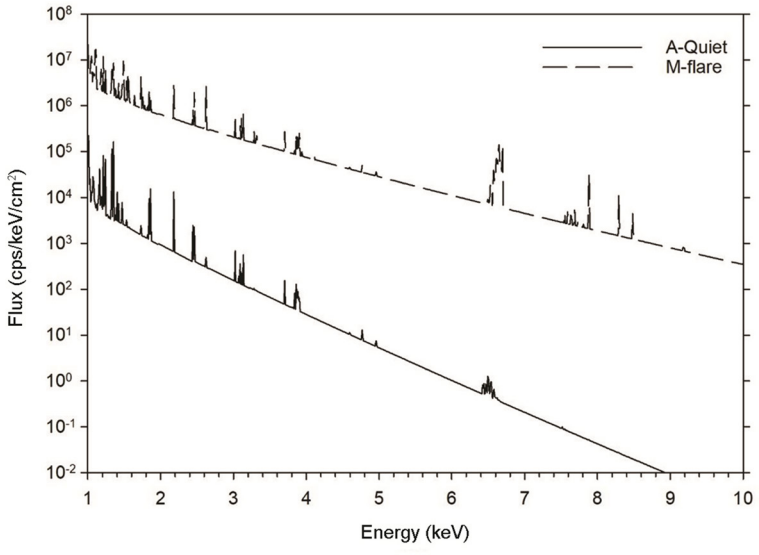

Figure 1. Solar X-ray spectra model used in the APXS calculations.

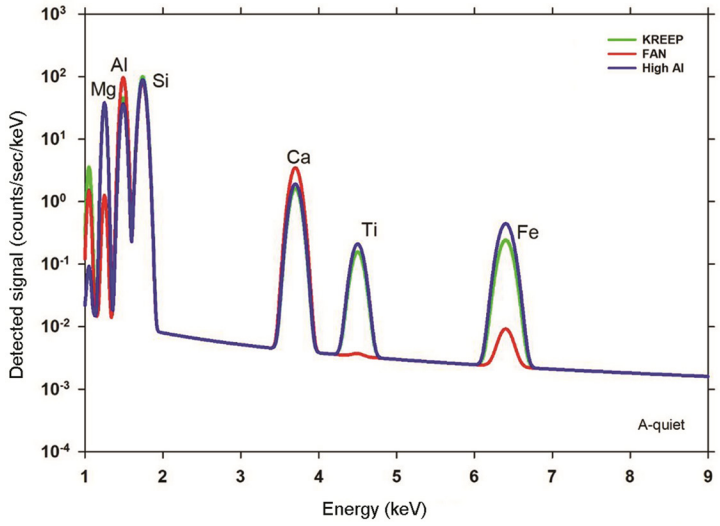

Figure 2. Modelled alpha particle-induced X-ray spectra for KREEP basalt, high Al basalt and FAN composition for solar A-quiet condition.

stopping power values and mass attenuation coefficients are obtained from NIST data.

The X-ray production cross-section has been experimentally estimated and discussed in several earlier studies for Al, Si, Mg, Ca, Ti and Fe[12–15]. In some studies, the theoretical K-shell ionization cross-sections are given and multiplied by the fluorescence yield of the element of interest to derive the X-ray production cross-sections. It may be noted that for some elements, the X-ray production cross-sections are not available for the entire alpha particle energy range 0.05–5.8 MeV and hence are based on extrapolation from the available cross-section data. For Na, the X-ray production cross-section varied from 40 to 2600 barn, whereas for Fe, it ranged between 0.15 and 180 barn, for alpha energies of 0.05–5.8 MeV.

The solar X-ray model was developed using collisional ionization equilibrium plasma, i.e. CIE model (previously known as MEKAL–Mewe–Kaastra–Liedahl) using the SPEX software (www.sron.nl/divisions/hea/spex), and appropriate emission measures and plasma temperatures in the CIE model. Figure 1 shows the modelled solar X-ray spectra for solar quiescent conditions. Mithun *et al.*[16] applied three power-law models defined over the respective energy ranges that are determined by two break energies for the continuum, whereas Clark and Trombka[1] have previously used solar models with a continuum shape but without line emission components. The X-ray scattered background component was explicitly determined using eq. (3) below, where f, r_e and θ are the atomic scattering factor, classical electron radius and scattering angle respectively. A Gaussian distribution was used to simulate the energy resolution of the X-ray detector.

$$I = C_j \frac{N}{A} \frac{r_e^2}{2} \frac{\Omega}{4\pi D^2} \times \int_{\lambda_{\min}}^{\lambda_{\text{edg}}} J(\lambda)\cos(\alpha)(1+\cos^2\theta) f^2 \times \frac{\mu_j(\lambda)\mathrm{d}\lambda}{\sum_i [C_i \mu_i(\lambda) + C_i \mu_i(\lambda_f)\cos\alpha/\cos\beta]}. \quad (3)$$

Figure 2 shows the modelled alpha particle-induced X-ray spectra for various lunar compositions, assuming a 30 mm^2 detector and a 30 mCi ^{224}Cm alpha source. For FAN composition, Al, Si, and Ca K_α lines can be clearly distinguished, and weaker Na and Fe K_α X-ray lines can be observed as well. In the case of KREEP basalt composition, Mg, Al, Si, Ca, Ti and Fe K_α lines are well above background levels, whereas the Na K_α X-ray line is also detectable. For the high Al basalt composition, all the major element K_α lines are well above the background, except the Na K_α line. In summary, the above modelling suggests that an alpha-induced X-ray spectrometer on a lunar lander (or rover) can observe K_α lines from major elements and distinguish different lunar compositions.

1. Clark, P. E. and Trombka, J. I., *J. Geophys. Res*., 1997, **102**, 16361–16384.
2. Banerjee, D. and Gasnault, O., *J. Geophys. Res*., 2008; doi:10.1029/2007JE003046.
3. Petro, N. E. and Pieters, C. M., *J. Geophys. Res*., 2004; doi:10.1029/2003JE002182.
4. Jenkins, R. and Devries, J., In *Practical X-ray Spectrometry*, Springer Verlag, New York, USA, 1967, p. 200.
5. Pillai, Netra S. and Narendranath, S., *Icarus*, 2021; 10.1016/j.icarus.2021.114436.
6. Narendranath, S. *et al*., *Adv. Space Res.*, 2014, **54**, 1993–1999.
7. Banerjee, D. and Vadawale, S. V., *Adv. Space Res.*, 2010, **46**, 651–656.
8. Rieder, R. *et al*., *J. Geophys. Res*., *Planets*, 2003, **108**, 8066.
9. O'Connell-Cooper, C. D. *et al*., *J. Geophys. Res*., *Planets*, 2017, **122**, 2623–2643.
10. Shanmugam, M. *et al*., *Curr. Sci.*, 2020, **118**, 53–61.
11. Clayton, E. *et al*., *Nucl. Instrum. Methods*, 1981, **180**, 541–548.
12. Lapicki, G., *J. Phys. Chem. Ref. Data*, 1989, **18**, 111.
13. Yu, Y. C. *et al*., *Phys. Rev. A*, 1991, **44**, 7252–7257.
14. Tribedi, L. C. and Tandon, P. N., *Phys. Rev. A*, 1992, **46**, 4425–4428.
15. Rutledge, C. H. and Watson, R. L., *At. Data Nucl. Data Tables*, 1973, **12**, 195–216.
16. Mithun, N. P. S. *et al*., *Planet. Space Sci.*, 2020; doi.org/10.1016/j.pss.2020.104923.

Received 19 January 2023; revised accepted 1 January 2024

DEBABRATA BANERJEE

Planetary Sciences Division,
Physical Research Laboratory,
Ahmedabad 380 009, India
e-mail: deba@prl.res.in